Using a Theoretical Model to Assess the Impact of Vascular Risk Factors on Autoregulation in the Retina

Brendan C. Fry,[1] Julia C. Arciero,[2] Croix Gyurek,[2] Amanda Albright,[2] Brent Siesky,[3] Alice Verticchio,[3] and Alon Harris[3]

[1]Department of Mathematics and Statistics, Metropolitan State University of Denver, Denver, Colorado, United States
[2]Department of Mathematical Sciences, Indiana University Indianapolis, Indianapolis, Indiana, United States
[3]Department of Ophthalmology, Icahn School of Medicine at Mount Sinai Hospital, New York, New York, United States

Correspondence: Julia C. Arciero, Department of Mathematical Sciences, Indiana University Indianapolis, 402 North Blackford Street, LD 270H, Indianapolis, IN 46202, USA;
jarciero@iu.edu.

Received: August 20, 2024
Accepted: December 13, 2024
Published: January 17, 2025

Citation: Fry BC, Arciero JC, Gyurek C, et al. Using a theoretical model to assess the impact of vascular risk factors on autoregulation in the retina. *Invest Ophthalmol Vis Sci.* 2025;66(1):42.
https://doi.org/10.1167/iovs.66.1.42

Purpose. Vascular impairments, including reduced capillary density (CD), impaired autoregulation capacity (Reg), and elevated intraocular pressure (IOP), have been identified as significant contributors to glaucomatous disease. This study implemented a theoretical model to quantify the impact of these impairments on retinal blood flow and oxygenation as intraluminal pressure (P_a) is varied.

Methods. A theoretical model of the retinal vasculature was used to simulate reductions in CD by 10% (early glaucoma) and 30% to 50% (advanced glaucoma), a range in autoregulation capacity from 0% (totally impaired) to 100% (totally functional), and normal (15 mm Hg) and elevated (25 mm Hg) levels of IOP.

Results. Under baseline conditions of CD = 500 mm^{-2}, Reg = 100%, and IOP = 15 mm Hg, an autoregulation plateau was predicted for P_a = 28 to 44 mm Hg. Decreased CD, impaired flow regulation mechanisms, and increased IOP all cause a loss of the autoregulation plateau and a corresponding decrease in tissue oxygenation in this pressure range. Although the detrimental effects of small decreases in CD or elevations in IOP are mostly offset by functional flow regulation, larger changes and/or combinations of vascular impairments lead to a significant drop in retinal oxygenation.

Conclusions. Model predictions indicate that isolated or combined vascular impairments in CD, flow regulation, and IOP contribute to poor retinal tissue oxygenation, which could lead to vision loss in advanced glaucoma patients. This study motivates early identification of vascular changes to prevent a substantially worse effect of these factors on retinal oxygenation during the progression of glaucoma.

Keywords: autoregulation, retinal blood flow, mathematical modeling, glaucoma, oxygenation

Primary open-angle glaucoma (POAG) is a multifactorial disease with high individual variability in risk factors. Although the treatment of elevated intraocular pressure (IOP) in POAG patients is well established, impairments in ocular blood flow and autoregulation[1] are also significant contributors to glaucomatous disease. However, such hemodynamic risk factors are not currently included in the standard of POAG care due to a lack of specific data demonstrating vascular insults as primary drivers of disease progression. Along with their individual importance in POAG, IOP, blood pressure (BP), and ocular hemodynamics are interwoven biomarkers where the combined effects of intra- and extravascular pressures on blood flow are not well understood.

Autoregulation is the process by which blood flow is maintained relatively constant over a wide range of intraluminal pressure. As arterial pressure is increased, the vascular smooth muscle tone in resistance vessels (arterioles) increases to yield decreased vessel diameter and increased vascular resistance. This intrinsic ability of the vasculature to autoregulate is a protective process to maintain homeostasis over the physiological arteriolar pressure range. Impaired autoregulatory ability occurs when blood flow does not remain relatively constant over varied physiological pressures. Several studies have demonstrated the importance and role of autoregulation in the retina and optic nerve head (ONH).[2–7] Specifically, POAG patients have been shown to exhibit faulty autoregulation of central retinal artery (CRA) blood flow during posture change.[7] In addition, patients with POAG under hypercapnia have been shown to lack vasodilatory response in the CRA, whereas subjects with ocular hypertension have demonstrated significantly increased volumetric blood flow to the retina.[6] These data suggest that patients with POAG have insufficient vascular autoregulation during physiological challenges that may result in decreased volumetric blood flow to the retina.

Mathematical modeling has been used to predict the impacts of impaired autoregulation on blood flow and oxygenation in many different tissues and organs. Carlson

et al.[8] included mechanistic responses to pressure, shear stress, and metabolism to predict changes in vessel diameters and downstream oxyhemoglobin saturation in a compartmental model of skeletal muscle. Arciero et al.[9] adapted and re-parameterized this model for application to the retina, but predictions were still made within a compartmental network geometry. Ursino et al.[10,11] developed several compartmental models of the cerebral vasculature to identify relationships among cerebral blood flow, cerebral blood volume, intracranial pressure, and the action of cerebrovascular regulatory mechanisms. Though not in the eye and still within the context of a compartmental or electrical circuit model, the model accounted for a difference in pressure environment due to cerebral spinal fluid (CSF) pressure. Aletti et al.[12] provided an initial model of autoregulation in the context of a three-dimensional network of 25 segments of retinal arteries. The model included time-dependent Stokes equations for flow and mechanical principles for the endothelium and smooth muscle fibers, including a sigmoidal function for smooth muscle contraction. In the present study, elements from each of these studies, including vessel wall mechanics, IOP environment, and heterogeneous retinal network structure, were incorporated into a comprehensive, hybrid mathematical model to investigate the impact of vascular impairments on blood flow autoregulation.

Mathematical modeling is a proven tool to unravel individual and combined mechanisms that contribute to the pathophysiology of POAG. A wealth of studies has indicated that impaired blood flow regulation capacity, elevated IOP, fluctuations in BP and CSF, and decreased capillary density (CD) are associated with POAG.[13] Such impairments alter the normal capacity for flow autoregulation in glaucoma and cause a detrimental impact on retinal and ONH tissue oxygenation. In this study, blood flow is simulated within a realistic, heterogeneous description of a human retinal microvascular network. The mathematical model can be used to predict the impact of reductions in CD, impairments in autoregulation capacity, and increases in IOP on retinal blood flow and oxygenation as the incoming pressure is varied. This autoregulatory model is among the first to integrate each previously reported feature set into a single comprehensive model of retinal vascular autoregulation in POAG.

Methods

Theoretical Model of the Retina

Hybrid Geometry. The theoretical model of the retina that our group developed previously[14,15] is referred to as a hybrid model because it combines a heterogeneous network structure for arterioles with compartments for capillaries and venules. The heterogeneous arteriolar network structure was obtained from murine confocal microscopy images scaled appropriately to human.[11] A series of resistors (compartments) representing capillaries, small venules, and large venules is connected downstream of each terminal arteriole of the heterogeneous arteriolar network (see Fig. 1). The spatial heterogeneity of the arterioles is preserved in the downstream compartments because fractional flows based on oxygenation levels are calculated for each set of vessel compartments. Although blood is supplied to the human retina via four main arteries, only one of the four arteries is simulated to preserve computation time. Figure 1 provides a depiction of the vascular network geometry.

Hemodynamics. In the hybrid model, the microvascular network is represented as a directed graph, with the edges of the graph representing the vessels of the network and the nodes representing the network junctions. Blood flow through each of the vessels is assumed to be pressure driven and governed by Poiseuille's law:

$$Q = \Delta P \frac{\pi D^4}{128\,\mu L} \tag{1}$$

where Q is the blood flow rate, ΔP is the pressure drop along the vessel, D is the vessel diameter, μ is the apparent viscosity of the blood, and L is the vessel length.

The BP entering the arteriolar network was assumed to be 40 mm Hg,[9,16] and the venous output pressure was assumed to be the same as the IOP, initially set to 15 mm Hg. Given these boundary conditions, together with Poiseuille's law and assuming conservation of mass at each of the network junctions, an iterative process was used to solve for the interior flow, hematocrit, and apparent viscosity in all of the network vessels.[17,18]

Flow Regulation Mechanisms. According to the law of Laplace, circumferential tension (T) within the vessel wall is related to vessel diameter (D) and transmural

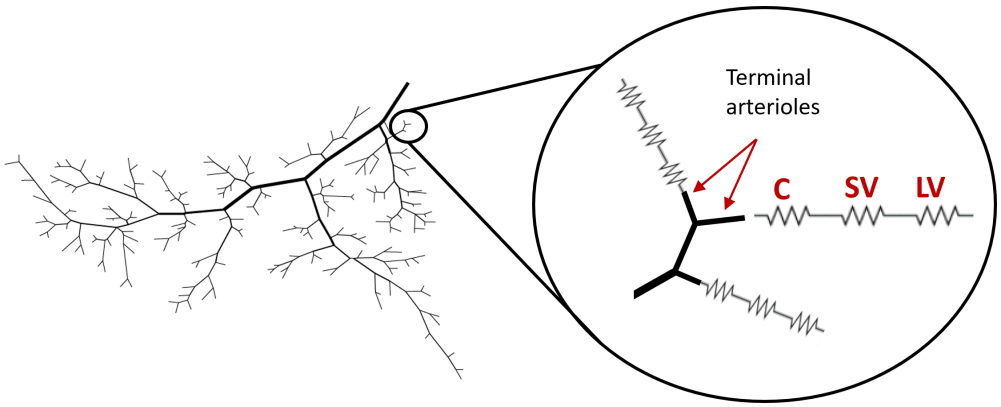

Figure 1. Schematic of network geometry of one branch of the retinal vasculature. The heterogeneous representation of the arterioles and compartmental representation of the capillaries (C), small venules (SV), and large venules (LV) together comprise the hybrid model. The circled region provides an enlargement to depict how a series of compartments is attached to each terminal arteriole.

pressure—that is, the difference between the pressure inside the vessel (P_{in}) and the pressure outside the vessel (P_{out})—by the following relationship, assuming vessel wall thickness is much smaller than vessel diameter: $T = \frac{(P_{in}-P_{out})D}{2}$. To account for the role of blood flow regulation, a vessel wall mechanics model is used here, as in our previous work,[8,9,19,20] in which total tension (T_{total}) within the vessel wall is modeled as the sum of passive tension (T_{pass}), due to structural components and modeled by an exponential function of diameter, and active tension, due to contraction of smooth muscle cells and modeled by the product of a Gaussian function of diameter representing the maximally active tension generated by smooth muscle (T_{act}^{max}) and the activation (A) of vascular smooth muscle:

$$T_{total} = T_{pass} + AT_{act}^{max} \tag{2}$$

where

$$T_{pass} = C_{pass} \exp\left[C'_{pass}\left(\frac{D}{D_0} - 1\right)\right] \tag{3}$$

and

$$T_{act}^{max} = C_{act} \exp\left[-\left(\frac{\frac{D}{D_0} - C'_{act}}{C''_{act}}\right)^2\right] \tag{4}$$

where D_0 is the passive vessel diameter at a pressure of 40 mm Hg.

In Equations 5 and 6, total activation (A_{total}) is assumed to vary between 0 and 1 and is modeled as a sigmoidal function of S_{tone}, which is the stimulus that dictates the amount of vascular smooth muscle tone that is generated. In this study, three blood flow regulation mechanisms are assumed to contribute to the generation of smooth muscle tone: the myogenic (pressure) response, shear stress (flow) response, and conducted metabolic (PO_2) response.

$$A_{total} = \frac{1}{1 + \exp(-S_{tone})} \tag{5}$$

where

$$S_{tone} = C_{myo}(T - T_{cs}) - C_{shear}\left(\tau_{wall} - \tau_{wall,cs}\right) - C_{meta}\left(S_{meta} - S_{meta,cs}\right) \tag{6}$$

In Equation 6, T, τ_{wall}, and S_{meta} represent the current values of tension, shear stress, and metabolic signal in a given vessel, respectively; T_{cs}, $\tau_{wall,cs}$, and $S_{meta,cs}$ represent the control state values (i.e., baseline conditions corresponding to a healthy human retina) of tension, shear stress, and metabolic signal in a given vessel, respectively. Changes in pressure, flow, and oxygen levels thus cause a change in smooth muscle activation and lead to the constriction or dilation of arteriolar diameters.

A system of ordinary differential Equations 7 and 8 is used to represent the rapid passive change in diameter followed by active smooth muscle contraction or relaxation to a new equilibrium diameter and activation in the ith arteriole:

$$\frac{dD_i}{dt} = \frac{1}{\tau_d}\frac{D_{cs,i}}{T_{cs,i}}(T_i - T_{total,i}(D_i, A_i)) \tag{7}$$

$$\frac{dA_i}{dt} = \frac{1}{\tau_a}\left(A_{total,i}(D_i, A_i) - A_i\right) \tag{8}$$

where τ_d and τ_a are time constants, and $D_{cs,i}$ is the control (reference) state diameter. Parameter values for the flow regulation model have been validated and estimated in previous modeling studies[9,15,19–21] and are given in the Table.

Oxygen Transport. Oxygen transport to tissue is modeled via the conservation of mass, which states that oxygen diffusion must equal oxygen consumption:

$$D_{diff}\alpha\nabla^2 P_{O2} = M(P_{O2}) \tag{9}$$

where D_{diff} and α are the diffusivity and solubility of oxygen in the tissue, respectively, and $M(P_{O2})$ is the tissue oxygen consumption rate. It is assumed here that $D_{diff}\alpha = 6 \times 10^{-10}$ cm^3 O_2/cm/s/mm Hg.[22,23] A Green's function method is used to solve Equation 9 in the arteriolar network and surrounding tissue.[17,24,25] In this method, vessels are modeled as discrete oxygen sources, and the tissue regions are considered oxygen sinks. The PO_2 at any given tissue point is calculated by summing the oxygen fields (Green's functions) produced by the surrounding sources and sinks. The Green's function method is especially useful because it can be applied to heterogeneous vascular network structures and allows for diffusive interaction among all vessel and tissue points.

In the capillary compartments, Equation 9 is solved using a Krogh cylinder model[26] as in Albright et al.[14] and Fry et al.,[27] whereby each capillary delivers oxygen via diffusion to a surrounding tissue sleeve. Oxygen exchange in the venules is neglected, as oxygen is primarily exchanged in the arterioles and capillaries. In each vessel segment, the conservation of mass dictates that the rate of change of the convective oxygen transport rate is equal to the rate of diffusive oxygen efflux per vessel length, as in Albright et al.[14]

Simulated Hemodynamic Impairments

In our clinical observations,[28] early POAG patients are shown to exhibit ~10% reduction in CD compared to healthy individuals, with advanced patients experiencing significant further reductions. Thus, decreases in CD from a baseline of 500 mm^{-2} ranging from 10% (early POAG) to 30% to 50% (advanced POAG) are simulated. Decreased CD corresponds to a larger Krogh cylinder surrounding the capillaries and leads to increased tissue regions experiencing reduced oxygenation, as described in our recent work.[27]

To model impairments to autoregulation mechanisms, a factor is multiplied in front of the myogenic (C_{myo}), shear (C_{sbear}), and metabolic (C_{meta}) terms in the stimulus equation (Equation 6) and is assumed to be a percentage that varies between 0% and 100%, where a value of 100% indicates fully functional flow regulation (herein defined as autoregulation capacity, Reg), and Reg = 0% indicates fully impaired autoregulation capacity.

Increased IOP is an established risk factor for POAG[29] and thus was elevated in this study to assess its impact on retinal blood flow and oxygenation in isolation and in combination with changes to CD and Reg. Baseline IOP is assumed to be 15 mm Hg, and elevated IOP is simulated at 25 mm Hg.

Table. Parameter Values for Flow Regulation Model

Description	Parameter	Value	Unit	Reference
VSM activation sensitivity	C_{myo}	$1.37/D_0$	cm/dyn	Fry et al.[21]
VSM shear stress sensitivity	C_{shear}	0.0258	cm^2/dyn	Fry et al.[21]
VSM metabolic sensitivity	C_{meta}	1000	1/μM/cm	Fry et al.[21]
Passive tension strength	C_{pass}	$1.67 \cdot D_0$	dyn/cm	Calculated
Passive tension sensitivity	C'_{pass}	$-0.027 \cdot D_0 + 12.52$	—	Fry et al.[21]
Maximum active peak tension	C_{act}	$1.30 \cdot D_0^{1.48}$	dyn/cm	Fry et al.[21]
Maximum active length dependence	C'_{act}	$-0.00146 \cdot D_0 + 1.13$	—	Fry et al.[21]
Maximum active tension range	C''_{act}	$-0.00146 \cdot D_0 + 0.308$	—	Fry et al.[21]
Passive reference diameter	D_0	29–151	μm	Calculated
Time constant for diameter	τ_d	1	s	Fry et al.[21]
Time constant for activation	τ_a	20	s	Fry et al.[21]
Control state diameter	D_{cs}	22–117	μm	Fry et al.[21]
Control state tension	T_{cs}	13–188	dyn/cm	Fry et al.[21]
Control state shear stress	$\tau_{wall,cs}$	1–260	dyn/cm^2	Arciero et al.[15]
Control state metabolic signal	$S_{meta,cs}$	0.05–0.20	μM·cm	Arciero et al.[15]

VSM, vascular smooth muscle.

Autoregulation is defined as the phenomenon by which blood flow is maintained relatively constant over a wide range of intraluminal pressure values. When autoregulation is functioning under healthy conditions, an increase in pressure should lead to an increase in tension, an increase in S_{tone} (Equation 6), an increase in activation (Equation 5), and thus a decrease in vessel diameter to maintain blood flow despite the increase in pressure. Simulations were conducted over a range of CD values, IOP values, and autoregulation capacities to determine the effects of impairments in these factors on the ability to maintain blood flow and oxygenation over a range of incoming arterial pressures.

Results

Under baseline conditions for CD and autoregulation functionality (i.e., CD = 500 mm^{-2} and Reg = 100%), an autoregulation plateau is predicted for incoming arterial pressure (P_a) values of P_a = 28 to 44 mm Hg in Figure 2A (blue line). Without the ability to regulate flow (Reg = 0%), the autoregulation plateau disappears completely (Fig. 2A, black line), and the predicted flow increases significantly with pressure, including for P_a = 28 to 44 mm Hg. Figure 2B shows the corresponding average downstream (post-capillary) oxygen saturation predicted by the model for the same conditions. When flow regulation mechanisms are fully functional (Reg = 100%), the plateau in flow between P_a of 28 and 44 mm Hg corresponds to a similar plateau in oxygen saturation over that range (blue line), with values dropping only 13.6% from P_a = 44 mm Hg to P_a = 28 mm Hg. In the absence of regulation (Reg = 0%), there is a much larger (90.3%) drop in oxygen saturation for that same pressure range (Fig. 2B). Outside the autoregulation range (i.e., for P_a > 44 mm Hg or P_a < 28 mm Hg), flow increases with pressure, as expected.

The impact of decreasing CD by 10% (450 mm^{-2}, black), 30% (350 mm^{-2}, red), and 50% (250 mm^{-2}, blue)

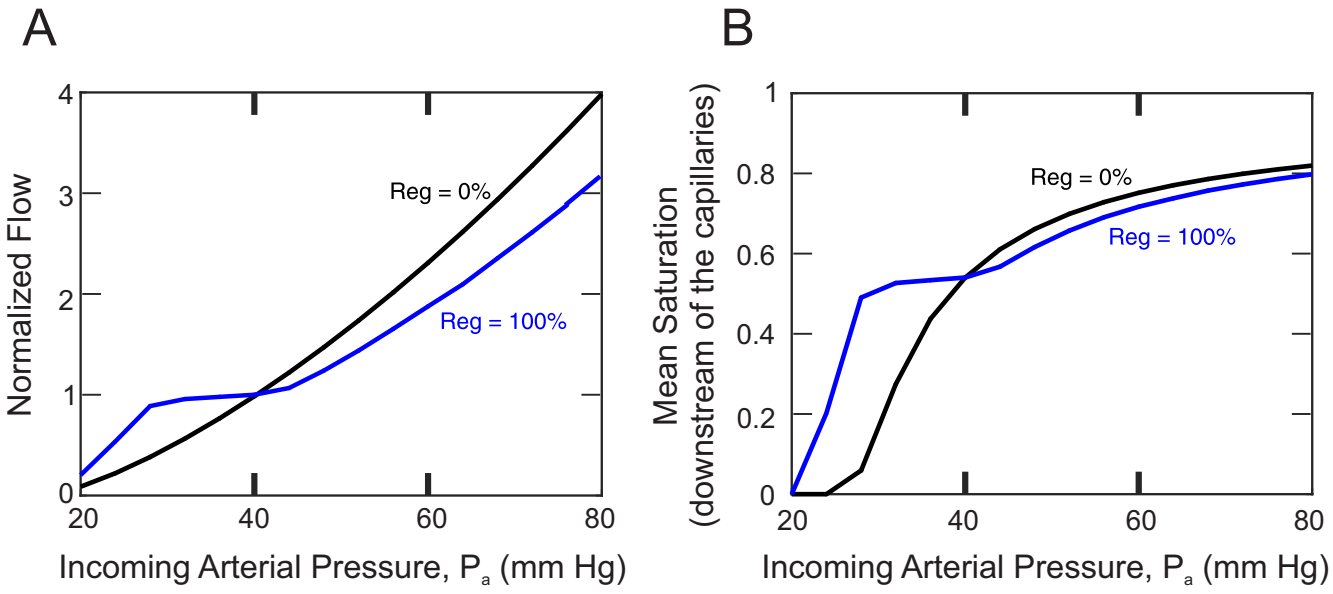

Figure 2. (**A**) Normalized flow as a function of P_a for Reg = 0% (*black*) and Reg = 100% (*blue*). (**B**) Mean downstream oxygen saturation as a function of P_a for Reg = 0% (*black*) and Reg = 100% (*blue*). These simulations assume IOP = 15 mm Hg and CD = 500 mm^{-2}.

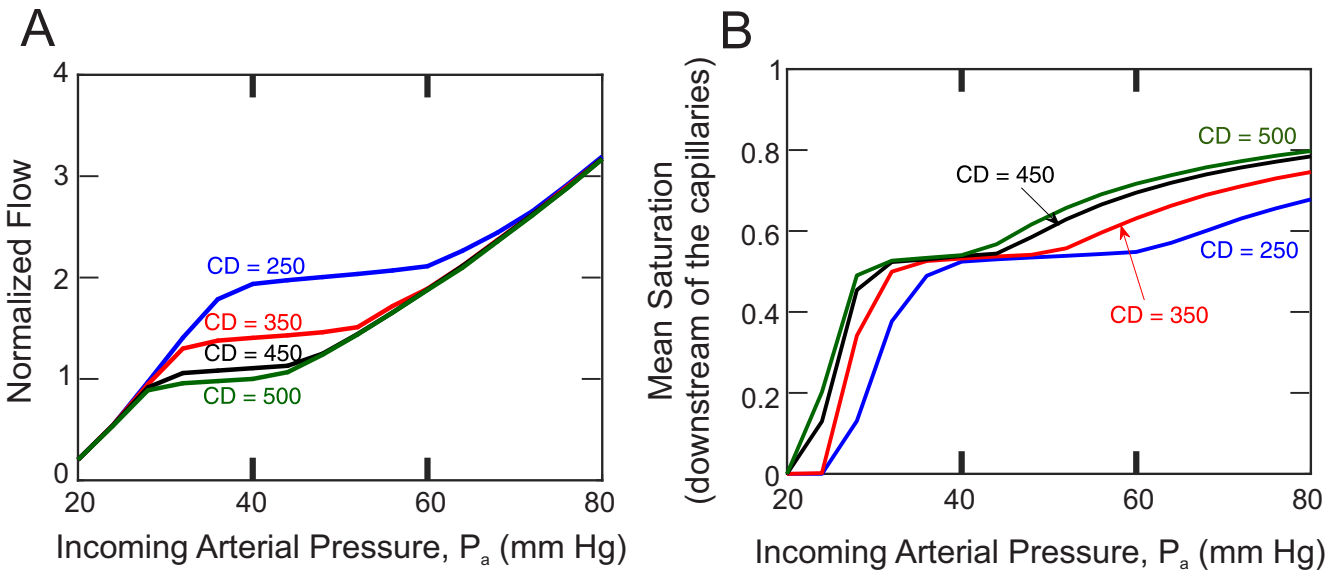

Figure 3. (**A**) Normalized flow as a function of P_a for CD = 500 mm^{-2} (*green*), 450 mm^{-2} (*black*), 350 mm^{-2} (*red*), and 250 mm^{-2} (*blue*). (**B**) Mean downstream oxygen saturation as a function of P_a for CD = 500 mm^{-2} (*green*), 450 mm^{-2} (*black*), 350 mm^{-2} (*red*), and 250 mm^{-2} (*blue*). These simulations assume IOP = 15 mm Hg and Reg = 100%.

is compared with the baseline case (500 mm^{-2}, green) in Figure 3. As CD is decreased, the autoregulation plateau is translated to higher pressure values, and flow levels are increased (Fig. 3A). Thus, significant decreases in CD lead to a loss in the autoregulation plateau in the normal physiological range of P_a = 28 to 44 mm Hg. The effects of decreased CD on downstream oxygen saturation are shown in Figure 3B; a loss in the ability to autoregulate leads to large decreases in oxygenation over that physiological pressure range. In particular, as P_a is lowered from 44 mm Hg to 28 mm Hg, the change in downstream saturation is 13.6% for CD = 500 mm^{-2} (as noted in Fig. 2B); however, this change in saturation increases as CD is decreased: 16.5% at CD = 450 mm^{-2}, 36.4% at CD = 350 mm^{-2}, and 75.3% at CD = 250 mm^{-2}. This occurs despite all blood flow regulation mechanisms being active, which is the case for all simulations in Figure 3.

Figure 4 demonstrates the impact of CD on mean tissue PO_2 levels downstream of the capillaries for autoregulation capacities (Reg) of 0%, 25%, 50%, and 100%. A 10% decrease in CD (from 500 mm^{-2} to 450 mm^{-2}) yields a 5% decrease in tissue PO_2, whereas total impairment of regulation when CD = 450 mm^{-2} yields an 8% decrease in tissue PO_2. If the CD is reduced by 10% *and* regulation is impaired, PO_2 in the tissue is decreased by 12.4%. For larger decreases in CD, the gap in oxygenation widens between cases with full and impaired regulatory capacity. From the base case of CD = 500 to 250 mm^{-2}, the decrease in predicted downstream tissue oxygenation is 46.5% when Reg = 100%, 50.7% when Reg = 50%, 60.9% when Reg = 25%, and 96.3% when Reg = 0%.

Because elevated IOP is a significant risk factor for glaucoma, the impact of increasing IOP on model predictions was also investigated. Figure 5 shows the predicted impact of increasing IOP from a baseline level of 15 mm Hg (blue) to an increased level of 25 mm Hg (red). In Figure 5A, the predicted impact of increased IOP on flow as a function of pressure is shown. Higher IOP is predicted to shift the

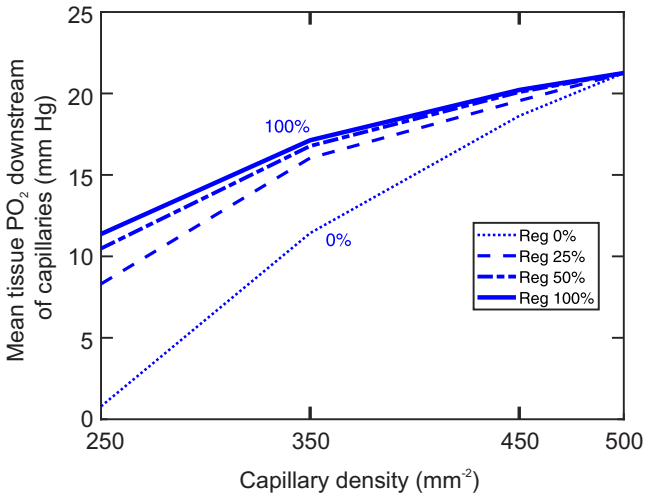

Figure 4. Mean tissue PO_2 levels downstream of the capillaries as CD is varied over four values: 250, 350, 450, and 500 mm^{-2}. Four levels of autoregulation capacity (Reg) are shown: 0% (*dotted*, fully impaired), 25% (*dashed*), 50% (*dash–dot*), and 100% (*solid*, fully functional). These simulations assume P_a = 40 mm Hg and IOP = 15 mm Hg.

autoregulatory curve to the right (i.e., to higher levels of P_a). The plateau is predicted to shift from P_a = 28 to 44 mm Hg for IOP = 15 mm Hg to P_a = 36 to 52 mm Hg for IOP = 25 mm Hg. The effects of this shift on downstream oxygen saturation are shown in Figure 5B. As expected, the shift of the flow plateau effectively shifts the oxygenation curve to the right, as well. Importantly, over the physiological range of P_a = 28 to 44 mm Hg, there is once again a loss in the autoregulatory plateau (in particular, for P_a < 36 mm Hg). As a result, the downstream oxygen saturation is predicted to be about 75.7% lower at P_a = 32 mm Hg with an IOP of 25 mm Hg than with an IOP of 15 mm Hg, and the satura-

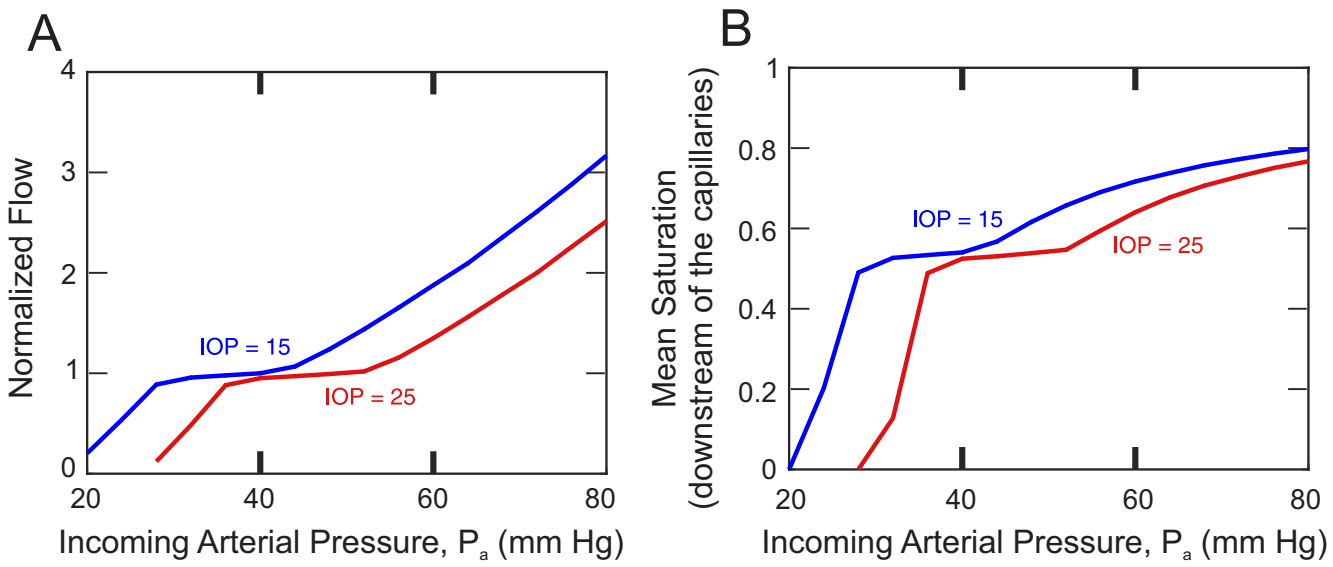

Figure 5. (**A**) Normalized flow as a function of P_a for IOP = 15 mm Hg (baseline, *blue*) and IOP = 25 mm Hg (high, *red*). (**B**) Mean downstream oxygen saturation as a function of P_a for IOP = 15 mm Hg (baseline, *blue*) and IOP = 25 mm Hg (high, *red*). These simulations assume CD = 500 mm^{-2} and Reg = 100%.

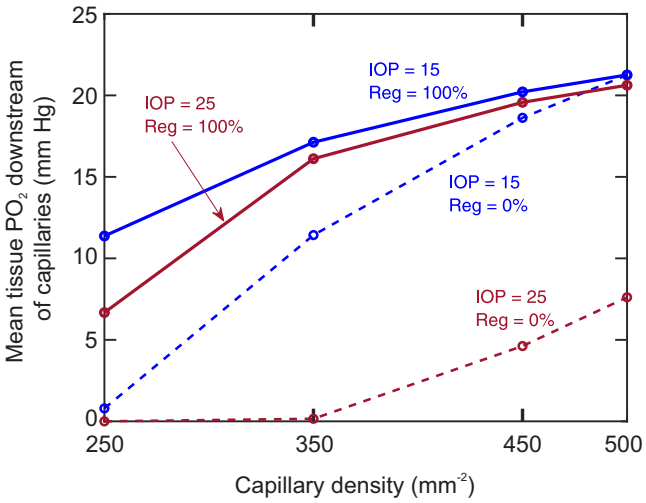

Figure 6. Mean tissue PO_2 levels downstream of the capillaries as CD is varied among four values: 250, 350, 450, and 500 mm^{-2}. Results are shown for a baseline IOP = 15 mm Hg and Reg = 100% (*blue*, *solid*), as well as IOP = 15 mm Hg and Reg = 0% (*blue*, *dashed*), IOP = 25 mm Hg and Reg = 100% (*red*, *solid*), and IOP = 25 mm Hg and Reg = 0% (*red*, *dashed*). These simulations assume P_a = 40 mm Hg.

tion is predicted to be near 0 for P_a = 28 mm Hg in the high IOP case.

To investigate the combined effects of elevated IOP and impaired blood flow regulation on tissue oxygenation, the model was simulated for a range of CD, with normal and high IOP, and with and without blood flow regulation. Figure 6 shows the predicted mean tissue PO_2 level downstream of the capillaries with combinations of IOP = 15 and 25 mm Hg and Reg = 0% and 100% over a range of CD. With fully functioning regulation mechanisms, an increase in IOP from 15 to 25 mm Hg leads to a predicted decrease in downstream tissue PO_2 from 21.3 mm Hg to 20.6 mm Hg with a baseline CD of 500 mm^{-2}. If CD is decreased to 250 mm^{-2}, the downstream tissue PO_2 is predicted to decrease to 11.4 mm Hg when IOP = 15 mm Hg and to 6.7 mm Hg when IOP = 25 mm Hg. This gap in predicted oxygenation levels between the baseline and elevated IOP cases is much higher (41.3%) at CD = 250 mm^{-2} compared to CD = 500 mm^{-2} (3%). The combination of high IOP and fully impaired flow regulation (red dotted line in Fig. 6) exacerbates the decreases in tissue PO_2 as CD is decreased, so that even a 10% reduction in CD (to 450 mm^{-2}) leads the predicted downstream tissue PO_2 to be just 4.6 mm Hg. Further reductions of CD to 350 and 250 mm^{-2} yield predicted downstream tissue PO_2 values of 0.2 mm Hg and 0 mm Hg, respectively, in the absence of flow regulation and with elevated IOP.

Discussion

A theoretical model of the human retinal microvasculature is used in this study to elucidate factors that impact autoregulation of blood flow within the retina. The model predicts that conditions observed in POAG patients such as decreased CD, impaired blood flow regulation mechanisms, and increases in IOP all lead to a loss of the autoregulation plateau in the physiological range of incoming arterial pressures between 28 and 44 mm Hg. The loss of this autoregulation plateau corresponds to a significant decrease in oxygenation in that pressure range. These model predictions are used to hypothesize that the inability to autoregulate could explain, at least in part, the loss of visual function in advanced glaucoma patients.

Our model indicated that reductions in CD translate the autoregulation plateau to higher pressure and flow values (see Fig. 3). Model predictions show a small change in the blood saturation levels at the downstream end of the capillaries when CD is reduced from 500 mm^{-2} to 450 mm^{-2}. However, this change in blood saturation downstream of the capillaries is much more significant when CD is reduced to 350 mm^{-2} and 250 mm^{-2}, leading to significant impair-

ments in oxygenation with capillary loss. Figure 4 shows that functional flow regulation mechanisms can compensate and address small changes in CD but are not sufficient to overcome the larger reductions.

When flow regulation mechanisms are completely impaired, the mechanisms are held at their control state values, causing $S_{tone} = 0$ and activation to be 0.5 in the Reg = 0% case. Because $S_{tone} = 0$ on the steepest part of the (sigmoidal) activation curve, even the slightest change from $S_{tone} = 0$ will have a very significant effect on activation, thus explaining that even a small ability to regulate flow leads to much better results than if regulation is impaired completely (see Fig. 4). Further changes in Reg lead to comparable changes in S_{tone}, but not as significant of changes in activation due to the nonlinearity in the activation versus S_{tone} curve.

The model predicts a shift in the autoregulation curve toward higher P_a values when IOP is increased from 15 mm Hg to 25 mm Hg (see Fig. 5). This leads to a loss in the autoregulatory plateau over the normal physiological P_a range, which causes a large drop in downstream vessel oxygen saturation. For example, when $P_a = 32$ mm Hg, there is an extreme drop in oxygen saturation when IOP is elevated from 15 to 25 mm Hg. Thus, although increased IOP has historically been related to structural changes in the retina, the model predictions presented in this study suggest that elevated IOP impacts blood flow and oxygenation to a large extent, suggesting a key role of IOP in leading to vascular problems in glaucoma patients.

The model demonstrates a more detrimental effect on retinal oxygenation when two or more known vascular phenomena of POAG (i.e., capillary loss, flow regulation impairment, and/or elevations in IOP) occur in combination. As expected, the predicted downstream tissue PO_2 decreases with decreasing CD in all cases, and there is a decrease in predicted downstream tissue PO_2 as IOP is increased from 15 mm Hg to 25 mm Hg. However, as CD is decreased, the gap between the normal and high IOP cases grows, as well. As noted in Figure 6, the difference between the tissue PO_2 for the high and low IOP cases grows from just 3% when CD = 500 mm^{-2} to 41% when CD = 250 mm^{-2}. The deleterious effects of elevated IOP on tissue oxygenation become exacerbated at lower levels of CD.

Limitations

By design, theoretical models are limited in their capacity to capture all factors that contribute to a physiological system. In this model, the network geometry accounts only for heterogeneity in arteriolar network structure, although fractional flows are assigned to capillary compartments to try to preserve the impact of vascular heterogeneity. However, the current (generalized) network geometry was not obtained from individual human patients. Future work will digitize patient-specific vascular network geometries obtained from ultrawide optical coherence tomography angiography imagery of blood vessel geometry. The model will be applied to those clinically obtained vascular geometries so that model predictions can be compared more accurately to other patient characteristics. For example, model predictions of tissue oxygenation will be validated with Zilia oximetry measures that will be obtained from each ocular quadrant of patients. Patient-specific network geometries may also help to illustrate whether inferior or superior regions of the eye are predicted to exhibit lower oxygen levels and help to establish a potential role of gravity on blood flow dynamics when comparing predicted oxygen levels with clinical visual field data. A blood flow steal phenomenon has also been suggested to occur in patients with vascular dysregulation where a shift in blood flow occurs between vascular beds as they attempt to compensate for local tissue insufficiency.[30] Future modeling studies of retinal hemodynamics should be designed where possible to account for the potential influence of gravity and autoregulatory factors along with differing blood vessel geometry.

Conclusions

Previous work has strongly associated individual physiological factors with POAG including elevated IOP, variations in BP and CSF, lower CD and blood flow, and lack of healthy vascular autoregulation. In the present study, the model demonstrates that combinations of impaired regulation, high IOP, and reduced CD all contribute to poor tissue oxygenation. If blood flow regulation mechanisms are functioning, the impact on tissue oxygenation is minimal when IOP is increased on its own or during a small (~10%) decrease in retinal CD. This model prediction thus motivates early identification of vascular changes to prevent a substantially worse effect of these factors on retinal oxygenation in the more advanced stages of glaucoma. Ultimately, whether from increased IOP (causing poor autoregulation), impaired blood flow regulation mechanisms, or decreased CD, the results indicate how vascular risk factors may lead to poor oxygenation outcomes consistent with POAG disease.

Acknowledgments

Supported by grants from the National Science Foundation (DMS-1654019, DMS-2150108 to JA); National Institutes of Health (R01EY030851 to JA, BF, AH, BS, AV; R01EY030851, R01EY034718 to AH); The Glaucoma Foundation; and Research to Prevent Blindness.

Disclosure: **B.C. Fry**, None; **J.C. Arciero**, None; **C. Gyurek**, None; **A. Albright**, None; **B. Siesky**, None; **A. Verticchio**, None; **A. Harris**, AdOM (C, F), Cipla (C), Oxymap (F), Qlaris Bio (C, F), SlitLED (F)

References

1. Harris A, Guidoboni G, Siesky B, et al. Ocular blood flow as a clinical observation: value, limitations and data analysis [published online ahead of print January 24, 2020]. *Prog Retin Eye Res*. 2020;100841.
2. Grunwald JE, Riva CE, Stone RA, Keates EU, Petrig BL. Retinal autoregulation in open-angle glaucoma. *Ophthalmology*. 1984;91(12):1690–1694.
3. Grunwald JE, Sinclair SH, Riva CE. Autoregulation of the retinal circulation in response to decrease of intraocular pressure below normal. *Invest Ophthalmol Vis Sci*. 1982;23(1):124–127.
4. Riva CE, Hero M, Titze P, Petrig B. Autoregulation of human optic nerve head blood flow in response to acute changes in ocular perfusion pressure. *Graefes Arch Clin Exp Ophthalmol*. 1997;235(10):618–626.
5. Riva CE, Sinclair SH, Grunwald JE. Autoregulation of retinal circulation in response to decrease of perfusion pressure. *Invest Ophthalmol Vis Sci*. 1981;21(1 pt 1):34–38.
6. Sines D, Harris A, Siesky B, et al. The response of retrobulbar vasculature to hypercapnia in primary open-

angle glaucoma and ocular hypertension. *Ophthalmic Res*. 2007;39(2):76–80.
7. Evans DW, Harris A, Garrett M, Chung HS, Kagemann L. Glaucoma patients demonstrate faulty autoregulation of ocular blood flow during posture change. *Br J Ophthalmol*. 1999;83(7):809–813.
8. Carlson BE, Arciero JC, Secomb TW. Theoretical model of blood flow autoregulation: roles of myogenic, shear-dependent, and metabolic responses. *Am J Physiol Heart Circ Physiol*. 2008;295(4):H1572–H1579.
9. Arciero J, Harris A, Siesky B, et al. Theoretical analysis of vascular regulatory mechanisms contributing to retinal blood flow autoregulation. *Invest Ophthalmol Vis Sci*. 2013;54(8):5584–5593.
10. Ursino M, Giulioni M, Lodi CA. Relationships among cerebral perfusion pressure, autoregulation, and transcranial Doppler waveform: a modeling study. *J Neurosurg*. 1998;89(2):255–266.
11. Ursino M, Lodi CA. Interaction among autoregulation, CO_2 reactivity, and intracranial pressure: a mathematical model. *Am J Physiol*. 1998;274(5 pt 2):H1715–H1728.
12. Aletti M, Gerbeau J, Lombardi D. Modeling autoregulation in three-dimensional simulations of retinal hemodynamics. *MAIO [Internet]*. 2016;1(1):88–115.
13. Verticchio Vercellin AC, Harris A, Oddone F, et al. Ocular blood flow biomarkers may predict long-term glaucoma progression. *Br J Ophthalmol*. 2024;108(7):946–950.
14. Albright A, Fry BC, Verticchio A, Siesky B, Harris A, Arciero J. Metabolic blood flow regulation in a hybrid model of the human retinal microcirculation. *Math Biosci*. 2023;357:108969.
15. Arciero J, Fry B, Albright A, et al. Metabolic signaling in a theoretical model of the human retinal microcirculation. *Photonics*. 2021;8(10):409.
16. Guidoboni G, Harris A, Cassani S, et al. Intraocular pressure, blood pressure, and retinal blood flow autoregulation: a mathematical model to clarify their relationship and clinical relevance. *Invest Ophthalmol Vis Sci*. 2014;55(7):4105–4118
17. Fry BC, Coburn EB, Whiteman S, Harris A, Siesky B, Arciero J. Predicting retinal tissue oxygenation using an image-based theoretical model. *Math Biosci*. 2018;305:1–9.
18. Young DM. Iterative methods for solving partial difference equations of elliptic type. *Trans Am Math Soc*. 1954;76:92–111.
19. Arciero JC, Carlson BE, Secomb TW. Theoretical model of metabolic blood flow regulation: roles of ATP release by red blood cells and conducted responses. *Am J Physiol Heart Circ Physiol*. 2008;295(4):H1562–H1571.
20. Fry BC, Harris A, Siesky B, Arciero J. Blood flow regulation and oxygen transport in a heterogeneous model of the mouse retina. *Math Biosci*. 2020;329:108476.
21. Fry BC, Roy TK, Secomb TW. Capillary recruitment in a theoretical model for blood flow regulation in heterogeneous microvessel networks. *Physiol Rep*. 2013;1(3):e00050.
22. Ellsworth ML, Popel AS, Pittman RN. Assessment and impact of heterogeneities of convective oxygen transport parameters in capillaries of striated muscle: experimental and theoretical. *Microvasc Res*. 1988;35(3):341–362.
23. Bentley TB, Meng H, Pittman RN. Temperature dependence of oxygen diffusion and consumption in mammalian striated muscle. *Am J Physiol*. 1993;264(6 pt 2):H1825–H1830.
24. Hsu R, Secomb TW. A Green's function method for analysis of oxygen delivery to tissue by microvascular networks. *Math Biosci*. 1989;96(1):61–78.
25. Secomb TW, Hsu R, Park EY, Dewhirst MW Green's function methods for analysis of oxygen delivery to tissue by microvascular networks. *Ann Biomed Eng*. 2004;32(11):1519–1529.
26. Krogh A. The number and distribution of capillaries in muscles with calculations of the oxygen pressure head necessary for supplying the tissue. *J Physiol*. 1919;52(6):409–415.
27. Fry BC, Gyurek C, Albright A, et al. Predicting the impact of retinal vessel density on retinal vessel and tissue oxygenation using a theoretical model. *Math Biosci*. 2024;377:109292.
28. Verticchio Vercellin A, Siesky B, Antman G, et al. Regional vessel density reduction in the macula and optic nerve head of patients with pre-perimetric primary open angle glaucoma. *J Glaucoma*. 2023;32(11):930–941.
29. Le A, Mukesh BN, McCarty CA, Taylor HR. Risk factors associated with the incidence of open-angle glaucoma: the visual impairment project. *Invest Ophthalmol Vis Sci*. 2003;44(9):3783–3789.
30. Costa VP, Kuzniec S, Molnar LJ, Cerri GG, Puech-Leao P, Carvalho CA. Collateral blood supply through the ophthalmic artery: a steal phenomenon analyzed by color Doppler imaging. *Ophthalmology*. 1998;105(4):689–693.

Investigative Ophthalmology & Visual Science